

Impact Behavior of Multi-Layered UHMWPE Vests Reinforced with Titanium and PVC for Ballistic Protection

Nabil Muzhaffar Effendi¹, Azhari Sastranegara^{1*}, Rendi Hernawan¹, Lydia Anggraini¹

¹ Mechanical Engineering Study Program, Faculty of Engineering, President University, Indonesia

Correspondence: E-mail: azhari.sastranegara@president.ac.id

ABSTRACT

Achieving lightweight and high-performance bulletproof vests is essential for military and law enforcement, where balancing mobility and ballistic resistance is critical. This study investigates the ballistic performance of multi-layered Ultra-High Molecular Weight Polyethylene (UHMWPE) vests reinforced with titanium (Ti6Al4V) and polyvinyl chloride (PVC). Two innovative vest configurations were evaluated following National Institute of Justice (NIJ) Standard-0101.04 ballistics tests and simulated using the Finite Element Method (FEM). Experimental findings indicated that while Vest 1 significantly absorbed impact energy, it failed to prevent projectile penetration. In contrast, Vest 2, incorporating additional titanium and polymer layers, effectively mitigated the penetration of 9 mm Full Metal Jacket (FMJ) projectiles while maintaining a safe back-face signature (BFS). The FEM simulation results demonstrated strong agreement with the experimental data, validating the effectiveness of multi-material layering in enhancing ballistic resistance. This research presents a strategic integration of titanium and polymer composites designed to achieve superior ballistic resistance while maintaining lightweight properties. These findings provided valuable insights for developing advanced body armor designs suitable for high-performance military and law enforcement applications.

ARTICLE INFO

Article History:

Received 13 Jan 2025

Revised 08 Feb 2025

Accepted 21 Feb 2025

Available online 14 Apr 2025

Keywords:

Ballistic impact test,

Bulletproof vest,

NIJ0101.04,

Numerical analysis,

UHMWPE,

1. INTRODUCTION

The increasing demands of modern warfare and law enforcement have highlighted the urgent need for lightweight yet highly effective body armor that offers su-

perior ballistic protection without compromising mobility and wearer comfort (Schart, 2023), (Magdi, 2019). Among the materials explored, Ultra-High Molecular Weight Polyethylene (UHMWPE) has emerged as a promising candidate due to its exceptional impact

resistance, high tensile strength, and low density (Bhatnagar et al, 2022), (Shelly et al, 2024). These properties make UHMWPE an ideal core material for ballistic applications. However, designing bulletproof vests that provide optimal protection against high-velocity impacts while maintaining flexibility, durability, and comfort remains a significant challenge (Asgedom et al, 2025).

Conventional body armor designs often struggle to balance lightweight construction with adequate protection against multi-impact scenarios or higher-caliber projectiles (Alil et al, 2018). While UHMWPE demonstrates excellent energy absorption capabilities, studies indicate that its standalone performance may be insufficient in mitigating blunt trauma or withstanding sustained high-velocity impacts (Alam et al, 2024), (Zhang et al, 2024), (Wang et al, 2024).

Research suggests that incorporating rigid reinforcements, such as ceramic or titanium layers, enhances penetration resistance; however, such configurations significantly increase weight and reduce mobility (Tsirogiannis et al, 2024), (Wu et al, 2024), (Andraskar et al, 2022). Additionally, integrating polymeric layers, such as polyvinyl chloride (PVC), has shown promise in reducing back face deformation and absorbing shock. However, the combined effects of UHMWPE, rigid materials, and polymeric layers remain underexplored (Lustig et al, 2025), (Wang et al, 2025).

To address these limitations, this study proposes a novel multi-layered bulletproof vest design that integrates UHMWPE, titanium (Ti6Al4V), and PVC layers. UHMWPE serves as the primary energy-absorbing material, titanium enhances penetration resistance, and PVC mitigates blunt trauma by distributing impact forces. This configuration aims to optimize ballistic performance while maintaining lightweight properties and wearer

comfort. The ballistic performance of these designs is evaluated through experimental testing following National Institute of Justice (NIJ) Standard-0101.04, using 9 mm Full Metal Jacket (FMJ) projectiles. Additionally, finite element simulations using LS-DYNA software are conducted to provide deeper insights into the behavior of multi-layered vests under ballistic impact.

2. METHODOLOGY

This study's methodology consists of five primary stages: material selection, vest design, experimental testing, numerical simulation, and comprehensive data analysis to compare results and formulate design recommendations. **Figure 1** illustrates the research flowchart. The primary materials used in this study include UHMWPE, Titanium Ti6Al4V, and PVC.

UHMWPE was selected as the core material due to its superior tensile strength and energy absorption properties, while Titanium Ti6Al4V was incorporated to enhance penetration resistance. PVC was included as a shock-absorbing layer to minimize blunt trauma. These materials were arranged in two vest configurations: a simpler configuration with fewer layers and an advanced configuration incorporating additional Titanium alloy and PVC layers.

The vest specimens used for the experimental tests were provided by PT. Cawisadi Aksatrya, a military parts manufacturer located in Jakarta. Prior to this research, the vests were designed and produced based on empirical experience. However, in this study, the vest design was further refined and discussed based on insights from recent research findings.

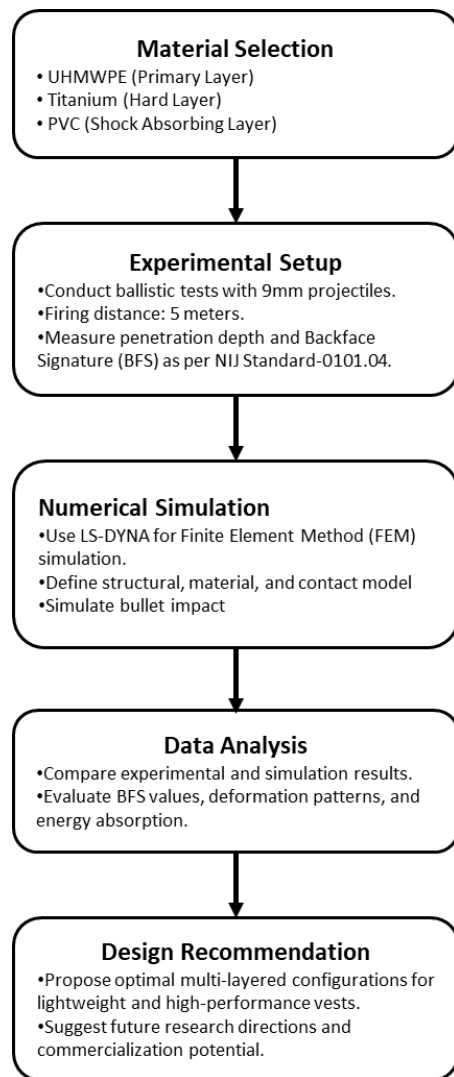


Figure 1. Research Flowchart

2.1. Material Selection and Vest Design

UHMWPE, a durable polymer known for its high tensile strength and impact resistance, serves as the primary material in this study. The UHMWPE fibers were obtained in yarn form, with their properties verified by Astra Otoparts Laboratory in Bekasi, West Java Province. The vest design also integrates Titanium Ti6Al4V as a rigid layer to improve penetration resistance and PVC as a shock-absorbing component (Pai *et al*, 2022).

These materials were used to construct two vest configurations:

- Vest 1

Vest 1 is a handmade, multi-layered vest with a total thickness of 7 mm. It consists of five layers of UHMWPE, two layers of PVC, and one layer of Titanium alloy. The arrangement of these layers was optimized to balance weight and ballistic resistance, ensuring effective energy absorption and impact dispersion. The total weight of Vest 1 is approximately 829 grams, with a cross-sectional area of 593 cm². **Figure 2** illustrates the layer arrangement of Vest 1, while **Table 1** details its dimensions and layer thickness. The numerical model representation of Vest 1 is shown in **Figure 3**.

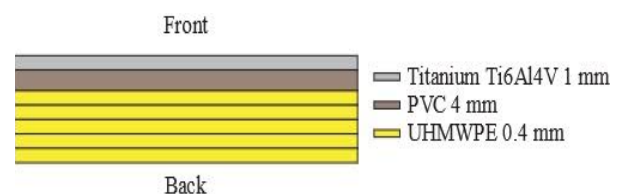


Figure 2. Structure of Vest 1

Table 1. Dimension of Vest 1

Material	Qty	Thickness (mm)	Weight (gr)
UHMWPE	5	0.4	829
PVC	1	3.4	
PVC	1	1	
Titanium	1	1	

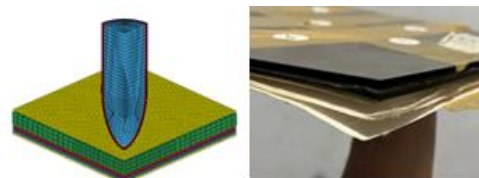


Figure 3. Vest 1 – Numerical Models and Prototypes

- Vest 2

Vest 2 is a multi-layered vest with a total thickness of 12 mm, comprising five layers of UHMWPE, two titanium plates, and two polymer layers, as illustrated in **Figure 4**.

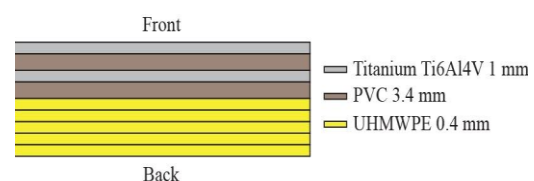


Figure 4. Structure of Vest 2

This configuration was specifically designed to improve ballistic resistance through layered reinforcement. The Titanium layers enhance durability and penetration resistance, while the PVC layers aid in dissipating impact energy. This design aims to improve bullet-stopping capability compared to Vest 1.

Vest 2 has a total weight of 980 grams. Its dimensions and layer composition are detailed in **Table 2**. **Figure 5** presents the numerical model representation of Vest 2, illustrating the structural arrangement used in simulations.

Table 2. Dimension of Vest 2

Material	Qty	Thickness (mm)	Weight (gr)
Titanium	1	1	980
PVC	1	3.4	
Titanium	1	1	
PVC	1	3.4	
UHMWPE	5	0.4	

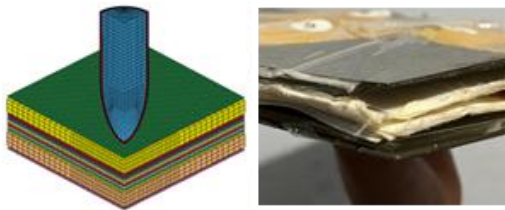


Figure 5. Vest 2 – Numerical Models and Prototypes

These vest designs were subjected to experimental and numerical analyses to assess their ballistic performance under impact from 9mm projectiles. The objective was to compare how each configuration absorbs impact energy and minimize back face deformation, providing insights into optimal layering for commercial applications.

2.2. Experimental Condition

The ballistic experiment was conducted at Indonesian Navy Main Weapons Laboratory (Laboratorium Induk Senjata LABINSEN, TNI-AL) located at Madura, East Java. The experiment was performed under controlled conditions following NIJ

Standard-0101.04 widely used for Level II Armor Protection category.

The experiment involved firing 9x19 mm Full Metal Jacket (FMJ) projectiles at test specimens using an STZA 12 mobile firing test platform. The platform was calibrated to launch projectiles at an initial velocity of 380 m/s measured by high-speed camera. Shots were fired from 5 meters at 0-degree impact angle. **Figure 6** illustrates the experimental test setup, while **Figure 7** presents a depiction of the bullet used. The projectile features a full metal jacket with a round-nose bullet, consisting of a Brass 72 (CuZn28) jacket and a Lead Antimony core. Detailed specifications of the firearm and ammunition are provided in **Table 3**.

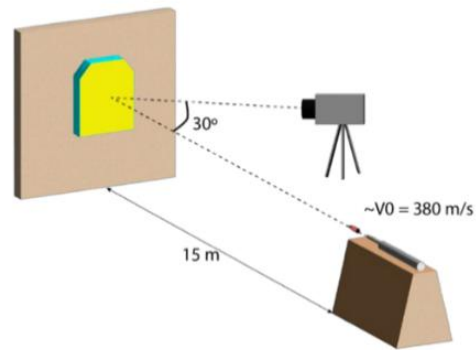


Figure 6. Illustration of experimental test setup



Figure 7. The 9mm bullet: A Cross-Sectional View and Dimensions

Table 3. Weapon Information

Specification	Details
Weapon Used	STZA 12 mobile firing test
Bullet Type	Pindad MU-1TJ 9x19mm FMJ
Velocity	380 m/s
Bullet Mass	12.26 grams
Shooting Distance	15 meters
Bullet Material	Brass 72 (CuZn28) jacket, Lead Antimony core
Total Length	29.70 mm
Gas Pressure	Max. 2600 kg/cm ²

The penetration depth of the bullets, commonly referred to as the back face signature (BFS), was recorded using a clay backing placed behind the vest. The BFS values provide insight into the level of blunt force trauma a wearer might experience. According to NIJ standards, BFS must not exceed 44 mm to prevent severe injury (Hanlon and Gillich, 2012).

2.3. Numerical Simulation Model

To simulate the experimental testing conditions, Finite Element Method (FEM) simulations were conducted using LS-Dyna®, employing an explicit method approach—a widely used technique for analyzing nonlinear phenomena and high-velocity impact deformations. These simulations were crucial for gaining deeper insights into complex material interactions under high-speed impact while overcoming the constraints of physical testing limitations (Zmindak *et al*, 2016)

The most appropriate material models were carefully selected to ensure the reliability of the simulation results. The details of the model and material properties used in this study are outlined below.

- Vest Model and Mesh Size:

The simulation model represented a quarter of the full vest structure to optimize computational efficiency. UHMWPE and Titanium layers were modeled using shell elements, while the PVC layer and the

bullet were modeled using hexahedral solid elements. Accurate meshing was critical for capturing high-stress regions, such as bullet entry points, and ensuring reliable simulation results. A finer mesh was applied to areas experiencing significant deformation to enhance the accuracy of penetration and impact assessments.

Although conducting a mesh independence test is essential in FEM simulations to ensure the reliability of results, the software license limitations imposed certain constraints. The use of an academic version of LS-DYNA restricted the number of nodes that could be utilized in the simulations. As a result, a comprehensive mesh independence test could not be performed. Instead, the mesh was refined to the highest resolution allowed by the available computing resources. This approach aimed to maximize simulation accuracy within the permissible limits of the software, especially in areas undergoing substantial deformation.

- Material Properties:

a. UHMWPE

The UHMWPE layer was modeled using MAT_FABRIC. As presented in **Table 4**.

Table 4. Mechanical Properties of the UHMWPE Layer for ADD_EROSION and MAT_FABRIC Material Models

Property	Value	Unit
Density, ρ	9.70e-09	Ton / mm ³
Young Mod. Longitudinal, EA	700	MPa
Young Mod.s Transverse, EB	700	MPa
Minor Poisson Ratio, ν_{BA}	0.33	-
Major Poisson Ratio, ν_{AB}	0.33	-
Shear Modulus, GAB	180	MPa
Rayleigh Damping, DAMP	0.1	%
Maximum Strain, ϵ_f	0.5	%

UHMWPE exhibits a density of 9.700e-09 Ton/mm³, a Young's modulus of 700 MPa, and a Poisson's ratio of 0.33, with a maximum strain limit of 0.5%. The

ADD_EROSION keyword was used to simulate material degradation under impact conditions. The material properties and material model for UHMWPE are taken from the work of Zhang et al (2020).

b. Titanium Alloy (Ti6Al4V)

The MAT_PIECEWISE_LINEAR material model with plasticity was used to simulate the titanium alloy's behavior. As shown in **Table 5**, the titanium alloy has a density of 4.430×10^{-8} Ton/mm³, a Young's modulus of 114 GPa, and a yield stress of 140 MPa. The Cowper-Symonds model was applied to capture strain rate sensitivity and dynamic response under high-velocity impact (Zhang et al, 2020).

Table 5. Mechanical Properties of Titanium Ti6Al4V for MAT_PIECEWISE_LINEAR_PLASTICITY Material Model

Property	Value	Unit
Density, ρ	4.430×10^{-8}	Ton / mm ³
Young Modulus, E	1.140×10^5	MPa
Poisson Ratio, ν	0.34	-
Yield Stress, SY	140	MPa
Tangent Modulus, ETAN	1.25	MPa
Failure Flag	0.54	-
Strain Rate Parameter, c	10	-

c. PVC

The PVC layer was modeled using MAT_PLASTICITY_POLYMER. As detailed in **Table 6**, PVC has a density of 1.100×10^{-9} Ton/mm³, a Young's modulus of 10 GPa, and Poisson's ratio of 0.38. The polymer's stress-strain behavior was defined for true strain, ensuring accurate modeling of both plastic and elastic responses under applied loads (Zhang et al, 2020).

Table 6. Mechanical Properties of Polymer for MAT_PLASTICITY_POLYMER Material Model

Property	Value	Unit
Density	1.100×10^{-9}	Ton / mm ³
Young Modulus	1.000×10^4	MPa
Poisson Ratio	0.38	-

d. Bullet

The mechanical properties and material model of the bullet are presented in **Tables 7** and **8**, respectively (Manes et al, 2014), (Zhang et al, 2020).

Table 7. Mechanical Properties of the Bullet

Property	Lead	Brass	Unit
Density	1.066×10^{-8}	8.52×10^{-9}	Ton/mm ³
Young Mod.	1.800×10^4	1.15×10^5	MPa
Shear Mod.	4900	4.00×10^4	MPa
Poisson Ratio	0.42	0.31	-

Table 8. Properties of the Bullet for MAT_JOHNSON_COOK Material Model

Property	Lead	Brass	Unit
A	1	111.69	MPa
B	55.551	504.69	MPa
N	0.098	0.42	-
C	0.230	0.009	-
M	1	1.68	-
D1	-	0	-
D2	-	2.65	-
D3	-	-(0.62)	-
D4	-	0.028	-
D5	-	0	-
Tm	760	988	K
Tr	293	293	K
ϵ_0	5.000×10^4	5.0×10^4	s ⁻¹
Cp	1.240×10^{10}	3.85×10^{10}	N mm / Ton K

The strain rate threshold during bullet compression was analyzed using the Grüneisen equation of state (EOS). The Grüneisen EOS parameters, as listed in **Table 9**, were adopted from the work of Manes et al (2020). This model accounts for strain- and temperature-sensitive plasticity, enabling precise simulations of lead and brass bullets.

Table 9. Grüneisen EOS Parameters of the Bullet

Property	Lead	Brass	Unit
C	2.028×10^6	3.834×10^6	mm/s
S1	1.627	1.429	-
γ_0	2.252	2000	-

The element types and material models used for each part of the vest and bullet are summarized in **Table 10**. The interaction between the bullet and the vest, as well as inter-layer contact within the vest, was simulated using the CONTACT_ERODING_SURFACE_TO_SURFACE algorithm. This approach allows for the removal of failed elements that no longer contribute to physical simulation, ensuring accurate ballistic impact modeling.

Table 10. Summary of Model Parts, Element Types, and Material Models for Vest 1 and Vest 2

Part Name	Element Model	Material Model
Titanium	Shell	MAT_PIECEWISE_LINEAR_PLASTICITY
Polymer PVC	Solid	MAT_PLASTICITY_POLYMER
UHMWPE	Shell	MAT_FABRIC
Bullet Jacket Model – Lead	Solid	MAT_JOHNSON_COOK
Bullet Jacket Model – Brass	Solid	MAT_JOHNSON_COOK

The primary objective of this simulation setup was to achieve accurate results while minimizing computational time through symmetry and optimized meshing. This approach provides a robust foundation for analyzing vest performance under ballistic impact by accurately representing the physics of high-speed projectile interactions and employing carefully selected material models.


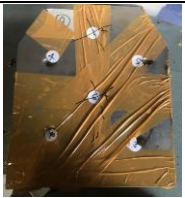


3. RESULTS AND DISCUSSION

3.1. Experimental Results

The ballistic performance of two vest configurations, Vest 1 and Vest 2, was experimentally evaluated under controlled conditions. Key metrics included BFS, structural deformation, and bullet-stopping capability. The deformed vests after ballistics tests and the BFS measurements, taken manually using a micrometer, are

presented in **Table 11**. The detailed results for each vest are discussed below.

Table 11. Specimen Final Deformation Condition

Specimen	Vest 1	Vest 2
Front Face		
Back Face		
Maximum BFS	Fully penetrated	18.1 mm
Minimum BFS	31.1	16.1 mm

From a total of six ballistics tests conducted on each vest, Vest 1 exhibited significant performance issues, with five complete penetrations where the bullets passed entirely through the vest. Only one bullet was successfully stopped by the vest, resulting in a Back face Signature (BFS) of 31.1 mm. In contrast, Vest 2 successfully halted all six bullets, demonstrating a 100% success rate. The BFS values recorded for Vest 2 ranged from a minimum of 16.1 mm to a maximum of 18.1 mm.

According to the NIJ Standard 0101.06 for Level II body armor, the maximum allowable BFS is 44 mm (Hanlon & Gillich, 2012). Comparing the experimental results with this criterion, the success rate of Vest 1 is approximately 17%, indicating that the vest fails to meet the required performance standards. The only non-penetrative impact still produced a BFS of 31.1 mm, which is below the threshold but inconsistent with the vest's overall performance.

On the other hand, Vest 2 exhibited a high degree of ballistic protection, with a BFS range of 16.1 mm to 18.1 mm, corre-

sponding to only 36% to 41% of the maximum allowable BFS under the NIJ standard. The results clearly demonstrate that Vest 2 is compliant with the standard and effectively mitigates blunt force trauma during ballistic impacts. The low and consistent BFS values further indicate a reliable material composition and manufacturing process.

3.2. Simulation Results

FEM simulations using the LS-DYNA explicit code were conducted to validate the experimental findings and provide insights into the dynamic behavior of multi-layered vests under ballistic impact. The deformation history of Vest 1 and Vest 2 is shown in **Table 12**. The results indicate that the bullet fully penetrated Vest 1, whereas Vest 2 successfully stopped the bullet. These findings align with the experimental results.

The simulation results were numerically validated using two criteria: artificial energy minimization and energy conservation throughout the simulation. The artificial energy generated, including sliding and hourglass energy, remained below 10%, meeting the accepted threshold. Energy conservation was assessed based on the energy ratio, which should be close to 1, as widely recognized in the literature (Signetti *et al*, 2022). The results presented in **Figures 8–11** confirm that the simulation exhibited minimal numerical errors and remained numerically stable.

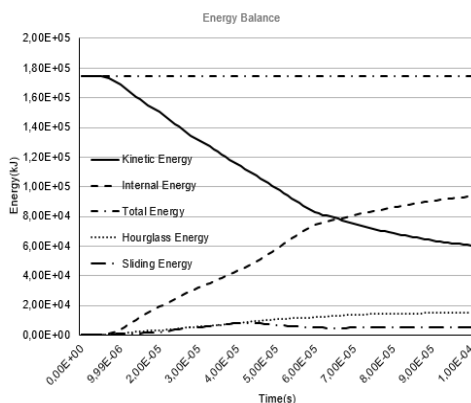
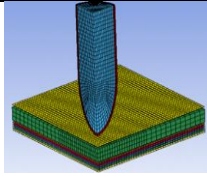
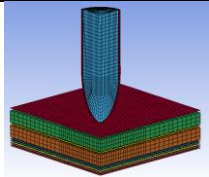
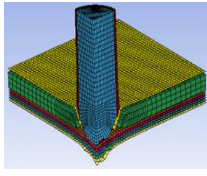
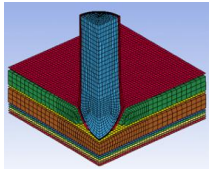
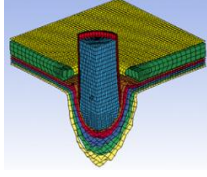
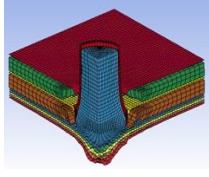
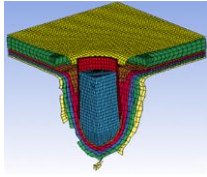
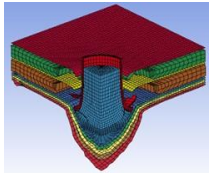
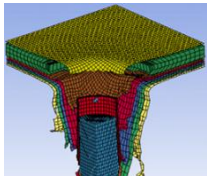
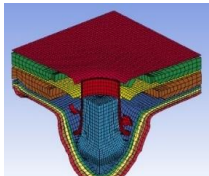


Figure 8. Vest 1 – Energy Balance

Table 12. Deformation History of Vest 1 (left) and Vest 2 (right)

Vest 1 (time step)	Vest 2 (time step)
	
0 s	0 s
	
2.019e-5 s	2.019e-5 s
	
4.038e-5 s	4.038e-5 s
	
6.059e-5 s	6.059e-5 s
	
8.078e-5 s	8.078e-5 s

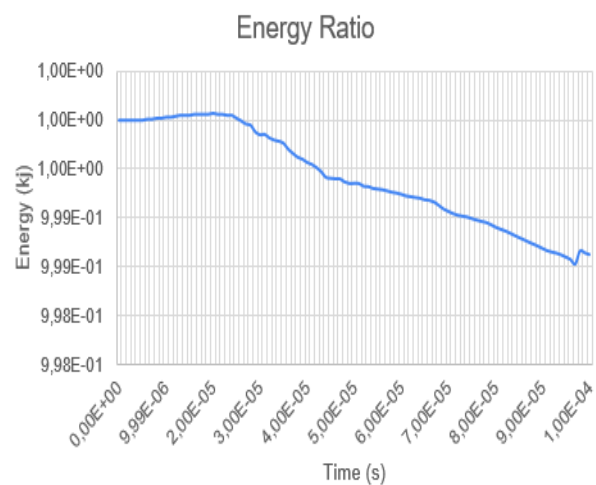


Figure 9. Vest 1 – Energy Ratio

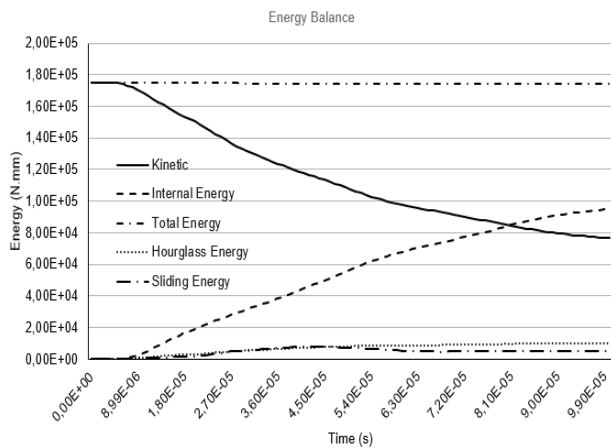


Figure 10. Vest 2 – Energy Balance

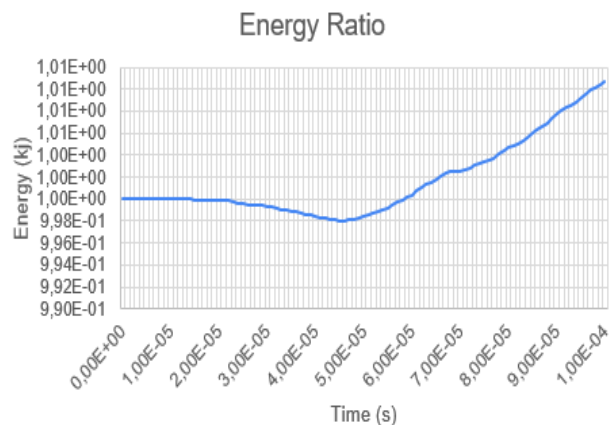


Figure 11. Vest 2 – Energy Ratio

The next step involves comparing the experimental and simulation results, which are presented sequentially for each vest as follows.

- Vest 1

The deformation comparison between the experimental and simulation results is shown in **Table 13**. In both cases, the bullet fully penetrated all layers.

Simulating the final deformation of UHMWPE layers is challenging due to the complexity of the phenomenon. However, the final bullet shape in the simulation closely matches the experimental results.

Table 13. Comparison of Experimental and Simulation Results for Vest 1

Layer	Mat	Experimental Results	Simulation Results
1	Titanium		
2	PVC		
3	UHMWPE		
4	UHMWPE		
5	UHMWPE		
6	UHMWPE		
7	UHMWPE		
Bullet	Brass & Lead		

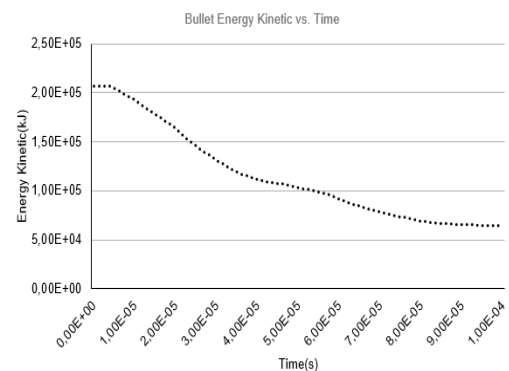


Figure 12. Vest 1 – Bullet's Kinetic Energy

The kinetic energy history in **Figure 12** shows a significant decrease throughout the simulation. However, the bullet was not stopped by the end of the simulation, which aligns with the evidence that it penetrated all layers.

- Vest 2

The deformation comparison between the experimental and simulation results is shown in **Table 14**. Both methods confirmed that the bullet was stopped within the vest. Similar to Vest 1, the deformed bullet in the simulation closely resembles the experimental results.

The kinetic energy history in **Figure 13** shows a more drastic decrease throughout the simulation. However, the bullet was not stopped by the end of the simulation, consistent with the evidence that it penetrated all layers.

The BFS comparison in **Table 15** shows that for Vest 1, the bullet fully penetrates all layers, meaning no BFS value is available. For Vest 2, the BFS values from the experimental results range from 15.90 mm to 16.40 mm, which closely aligns with the simulation result of 16.90 mm.










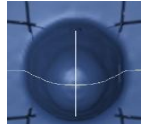
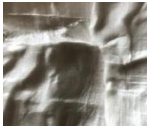
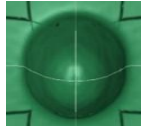

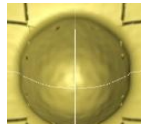

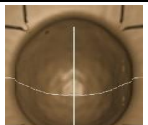

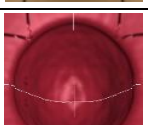

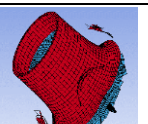
3.3. Comparative Analysis

The performance of Vest 1 and Vest 2 was evaluated across key metrics, including BFS, energy absorption, and bullet-stopping capability.

1. Back face Signature (BFS)

Vest 2 achieved BFS values well within NIJ standards, significantly outperforming Vest 1. The reduced BFS indicates a lower risk of blunt trauma for the wearer, making Vest 2 a more viable option for practical applications.

Table 14. Comparison of Experimental and Simulation Results for Vest 2

Layer	Mat	Experimental Results	Simulation Results
1	Titanium		
2	PVC		
3	Titanium		
4	PVC		
5	UHMWPE		
6	UHMWPE		
7	UHMWPE		
8	UHMWPE		
9	UHMWPE		
Bullet	Brass & Lead		

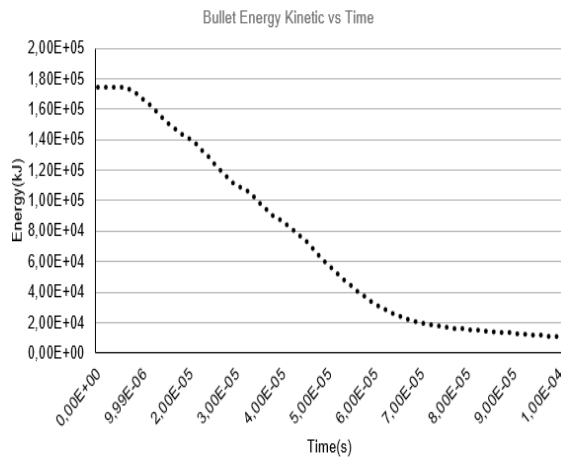
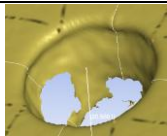
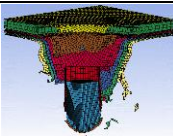




Figure 13. Vest 2 – Bullet's Kinetic Energy

Table 15. Comparison of BFS for Each Vest

Vest	Experiment BFS	Simulation BFS	Final Deformation
Vest 1	Min: N/A Max: N/A fully penetrated	 fully penetrated	
Vest 2	Min: 15.90 mm Max: 16.40 mm	 16.90 mm	

2. Energy Absorption and Bullet Stopping

Vest 2 demonstrated effectiveness in reducing bullet impact damage, successfully stopping all bullets, whereas Vest 1 failed to stop any. Experimental and simulation results confirmed that Vest 2 effectively utilized a combination of hard and soft layers. The functional analysis of each layer is as follows:

- **Layers 1 and 3** (hard layers): Reduce bullet velocity, disrupt, and deform it.
- **Layers 2 and 4** (soft layers): Retain bullet fragments and distribute impact energy.
- **Layers 5–9** (fiber layers): Absorb bullet energy and prevent further penetration. The effectiveness of the fiber layers is evident, as only 2 out of 6 bullets penetrated layers 5–7.

In contrast, experimental and simulation data for Vest 1 showed that although kinetic energy was significantly reduced, the bullets still penetrated all layers. This result confirms that Vest 1 is not suitable for practical use.

4. CONCLUSION

Ballistic test experiments were conducted following NIJ 0101.04 guidelines for both vests, with results compared to numerical simulations. Vest 1, composed of titanium, PVC, and ultra-high molecular weight polyethylene (UHMWPE), demonstrated a significant reduction in bullet kinetic energy but failed to fully stop the bullets, as indicated by BFS measurements. In contrast, Vest 2, which incorporated additional titanium and polymer layers, significantly improved energy absorption performance.

Vest 2 achieved a 100% success rate of halting the bullets, with its BFS ranging from 16.1 mm to 18.1 mm, which are 36% to 41% of the maximum allowable BFS. These BFS results are well within acceptable limits, affirming the armor's compliance with NIJ standards and its effectiveness in mitigating blunt force trauma from ballistic impacts. This finding highlights the importance of material combinations due to the distinct capabilities of each material.

The numerical models for both vests were consistent with the experimental results. This study also confirmed that the selected material models, contact models, and other FEM parameters were highly reliable and can be applied under similar conditions.

Further research is recommended to refine the design configuration, explore alternative materials, and evaluate the impact of higher-caliber ballistics.

ACKNOWLEDGEMENT

We thank PT. Cawisadi Aksatrya for providing the specimens used in this research. We also extend our gratitude to our colleagues from President University

for their valuable insights and expertise, which greatly contributed to this study, despite their disagreements with certain interpretations and conclusions presented in this paper.

REFERENCES

- Alam, S. and Aboagye, P. (2024). Numerical Modeling on Ballistic Impact Analysis of the Segmented Sandwich Composite Armor System. *Applied Mechanics*, 5(2), 340-362. <https://doi.org/10.3390/applmech5020020>.
- Alil, L., Matache and C., Sandu SM. (2018). Numerical Simulation of a Ballistic Impact on Tensylon® UHMWPE Laminates Using the Plastic Kinematic Model in LS-Dyna®. *Journal of Military Technology*, 1 (1). 43–50. <https://doi.org/10.32754/jmt.2018.1.08>.
- Andraskar, N.D., Tiwari, G., Goel, M.D. (2022). Impact response of ceramic structures - A review. *Ceramics International*, 48 (19), Part A. 27262-27279. <https://doi.org/10.1016/j.ceramint.2022.06.313>.
- Asgedom, G., Yeneneh K., Tilahun G., Negash, B. (2025). Numerical and experimental analysis of body armor polymer penetration resistance against 7.62 mm bullet. *Heliyon*, 11(1), e41286. <https://doi.org/10.1016/j.heliyon.2024.e412>.
- Bhatnagar, N., Prasad, S., Ram K., Kartikeya, K. (2022), Ballistic evaluation of steel/UHMWPE composite armor system against hardened steel core projectiles. *Int.Journal of Impact Engineering*, 164, 10211. <https://doi.org/10.1016/j.ijimpeng.2022.104211>.
- Hanlon, E. and Gillich, P. (2012). Origin of the 44-mm Behind-Armor Blunt Trauma Standard. *Military Medicine*, 177 (3), 333–339, <https://doi.org/10.7205/MILMED-D-11-00303>
- Lustig, M., Epstein, Y., Gefen, A. (2025). Plate materials for cardiopulmonary protection: a computational modeling study. *Computer Methods in Biomechanics and Biomedical Engineering*, 1–23. <https://doi.org/10.1080/10255842.2025.2476192>.
- Suchart, S. (2023). A review on lightweight materials for defence applications: Present and future developments. *Defence Technology*, 24, 1-17. <https://doi.org/10.1016/j.dt.2023.02.025>.
- Magdi, M. (2019). *Protective Armor Engineering Design* (1st ed.). New York: Apple Academic Press. <https://doi.org/10.1201/9780429057236>.
- Manes, A., Bresciani, L. M., Giglio, M. (2014). Ballistic performance of multi-layered fabric composite plates impacted by different 7.62 mm calibre projectiles. *Procedia Engineering*. 88. 208–215. <https://doi.org/10.1016/j.proeng.2014.11.146>.
- O'Masta, M.R., Compton, B.G., Gamble, E.A., Zok, F.W., Deshpande, V. S., Wadley, H.N.G. (2015). Ballistic impact response of an UHMWPE fiber reinforced laminate encasing of an aluminum-alumina hybrid panel. *Int. J. Impact Eng.*, 86. 131–144, <https://doi.org/10.1016/j.ijimpeng.2015.08.003>.
- Pai, A., Kini, C.R. and B., S.S. (2022). Development of materials and structures for shielding

- applications against Blast and Ballistic impact: A Detailed Review. *Thin-Walled Structures*, 179, p. 109664. <https://doi.org/10.1016/J.TWS.2022.109664>.
- Shelly, D., Lee, SY., Park, SJ. (2024). Compatibilization of ultra-high molecular weight polyethylene (UHMWPE) fibers and their composites for superior mechanical performance: A concise review. *Composite Part B: Engineering*, 275, 111924. <https://doi.org/10.1016/j.compositesb.2024.111294>.
- Signetti, S., Ryu, S., Pugno, N.M. (2022). Impact mechanics of multilayer composite armors: Analytical modeling, FEM numerical simulation, and ballistic experiments. *Composite Structures*. 297. 115916. <https://doi.org/10.1016/j.compstruct.2022.115916>.
- Tsirogiannis, E.C., Psarommatis, F., Prospathopoulous, A. (2024). Composite armor philosophy (CAP): Holistic design methodology of multi-layered composite protection systems for armored vehicles. *Defense Technology*, (41), 181-197. <https://doi.org/10.1016/j.dt.2024.07.009>.
- Wang, X., Zhang, R., Song, XT., Qiang, LS., Xu, X., Zheng, BQ. (2024). Ballistic performance of UHMWPE fiber laminates with pre-formed holes. *Thin-Walled Structures*, (201), Part B. 112011. <https://doi.org/10.1016/j.tws.2024.112011>.
- Wang, L., Kong, J., Chu, D., Wang, Y., Wang, T., Liu, Z. (2025). Enhancing ballistic performance: Effect of polyurea coating on backface deformation of UHMWPE laminates. *Composite Structures*, 355, 118846. <https://doi.org/10.1016/j.compstruct.2025.118846>.
- Wu, Y., Yu Y., Ma, M., Lu, W., Zhou, X., Wang, B., Gao, G. (2024). Numerical simulation of the penetration resistance of ceramic composite armor with corrugated structure. *Mechanics of Advanced Materials and Structures*, 1-17. <https://doi.org/10.1080/15376494.2024.2397096>.
- Zhang, R et al. (2020) Ballistic performance of UHMWPE laminated plates and UHMWPE encapsulated aluminum structures: Numerical simulation. *Composite Structure*, (252), 112686. <https://doi.org/10.1016/j.compstruct.2020.112686>.
- Zhang, R., Ni, CY., Zhang JH., Qiang LS., Zheng BQ. (2024). Multiple ballistic impacts of UHMWPE fiber metal laminates: Experiments and simulations. *Thin-Walled Structures*, (199), 111875. <https://doi.org/10.1016/j.tws.2024.111875>.
- Zmindak, M., Pelagic, Z., Pastorek, P., Mocilan, M., Vbostok, M. (2016). Finite Element Modelling of High Velocity Impact on Plate Structures. *Procedia Engineering*, 136. 162-168. <https://doi.org/10.1016/j.proeng.2016.01.191>.